# Ultra-Low-Power Multi-Sensor Fusion-Based Online Monitoring System for Fault Detection in Power Transmission Line Strain Clamps

Tiemin Zhao*, Wenpeng Li, Shiyang Zheng, Kai Li, Fangsen Chai, Shuang Ji
State Grid Jilin Electric Power Co., Ltd. Siping Power Supply Company, Siping 136000, China
E-mail: zzgjdw2025@163.com, 646729271@qq.com, 366377589@qq.com, 38727778@qq.com, chai8866@126.com, 1021295881@qq.com
*Corresponding author

**Keywords:** ultra-low-power, strain clamp, online monitoring, fault diagnosis, multi-sensor fusion

**Received:** October 15, 2025

*Failures of strain clamps on power transmission lines can undermine power system stability and disrupt electricity supply. To improve fault diagnosis accuracy, this study proposes an online monitoring approach based on a micro-power sensing device, employing a collaborative multi-sensor fusion framework for operating condition identification. Thermosensitive resonators, torque sensors, and strain gauges are used to collect temperature, resistance, torque, and deformation data, which are then fused using Support Vector Machines (SVM), Decision Trees, and Dempster–Shafer (D–S) evidence theory for fault classification. Laboratory tests involving 25,200 cases across seven measurement points showed that the proposed fusion model achieved an accuracy of 94.8% and an F1-score of 94.4%, representing improvements of 8.84% and 10.9%, respectively, over single-sensor models and outperforming baseline approaches. Field validation on 66 kV transmission lines operated by the State Grid Siping Power Supply Company confirmed its effectiveness in detecting major fault types such as clamp cracking, deformation, and bolt loosening. Furthermore, the predictive-assisted wake-up strategy effectively balanced energy consumption and response time, extending system endurance. Overall, the proposed method enhances diagnostic accuracy and energy efficiency, providing a practical solution for long-term online monitoring and smart grid applications.*

*Povzetek: Študija predstavlja energijsko varčen večsenzorski sistem za spletno zaznavanje napak nateznih sponk na daljnovodih z visoko diagnostično natančnostjo.*

## 1 Introduction

In modern power systems, transmission lines are essential for large-scale energy delivery and play a vital role in maintaining grid stability. Strain clamps transmit conductor tension and bear the primary mechanical load of the line, meaning their performance directly affects both tension balance and overall transmission safety [1–3]. With the rapid expansion of power grids, numerous strain clamp failures have been reported, including bolt loosening, aging, breakage, and localized overheating [4, 5]. If not detected in time, these faults can cause severe incidents such as conductor breakage, power outages, and even fires, leading to significant operational and safety consequences. Traditional inspection approaches are inefficient, offer limited coverage, and are prone to human error, making them inadequate for the increasing reliability demands of modern power systems [6–8].

Strain clamps are constantly exposed to harsh environments such as extreme temperatures, strong winds, rain, and snow. Their long-term service conditions are repeatedly influenced by mechanical stresses and climatic variations, resulting in loosening, fatigue, and heat buildup [9, 10]. National statistics indicate that overheating-related faults account for approximately 40% of failures in high-voltage electrical equipment. In one provincial grid, operational data from the past three years showed electricity losses of up to 465 MW caused by bolt loosening, overheating, and hardware deformation in strain clamps. These data underscore that strain clamps remain a critical weak point in transmission systems. Current detection methods still depend heavily on operator experience, leading to subjective and inconsistent assessments. As a result, they fail to provide reliable, long-term monitoring over the equipment's lifecycle, thereby increasing the overall risk of system failure [11–13].

To address the limitations of existing micro-power online monitoring technologies for transmission-line tension clamps—namely, weak single-parameter sensing capability, vulnerability of monitoring devices to failure, and low fault identification accuracy in multi-parameter fusion models—this study focuses on developing an intelligent monitoring system for tension clamps. A multi-parameter collaborative perception model is constructed, incorporating low-power sensors and an intelligent diagnostic platform to identify typical faults such as temperature rise, cracking, deformation, and bolt loosening. The core objectives of this study are threefold: (1) to verify whether an ultra-low-power multi-sensor fusion approach can improve fault detection accuracy by at least 10% compared with single-sensor models while maintaining energy efficiency; (2) to evaluate the effectiveness of the fusion strategy in optimizing energy consumption and response speed under different operating modes; and (3) to investigate the system's robustness and scalability under complex and extreme environmental conditions. The study encompasses four key aspects: monitoring architecture, sensing devices, data fusion modeling, and field experiments. The main innovations lie in the design of micro-power circuits and energy management mechanisms that enhance long-term operational stability, and the introduction of a multi-parameter fusion strategy that significantly improves fault identification performance. The results are expected to contribute to intelligent operation and maintenance of transmission lines, reduce accident risks, enhance power supply reliability, and accelerate the digital transformation of power grids.

## 2 Related work

In studies on the operational reliability of transmission lines, strain clamps are essential mechanical connectors whose failures can severely threaten line safety. Consequently, fault monitoring of strain clamps has attracted increasing research attention in recent years. Dadashizadeh Samakosh and Enayati [14] conducted experiments on a 63 kV overhead transmission line and established operational guidelines for strain clamps. Their results indicated that conductor surface overload leads to temperature increases, while non-standard crimping or repair sleeves under thermal stress may introduce potential defects. Chen et al. [15] observed that existing sag measurement systems exhibited low automation levels and that digital twin technologies for tensioned lines could not simulate operational conditions in real time. They developed an automated sag measurement device that improved on-site efficiency by 28%. Similarly, Luo et al. [16] employed an elastic catenary model combined with Fiber Bragg Grating (FBG) sensors to monitor sag and load under localized deformation, providing a theoretical basis for fault diagnosis in strain clamps.

Advances in intelligent sensing have facilitated the development of ultra-low-power technologies, offering new possibilities for the real-time monitoring of transmission line conditions. Li et al. [17] reviewed the applications of smart power sensors across generation, transmission, transformation, distribution, and utilization stages, highlighting future challenges for optical fiber, Micro-Electro-Mechanical Systems (MEMS), and self-powered sensors. Mai et al. [18] proposed a non-intrusive monitoring method for overhead lines by integrating uniaxial magnetic sensors, enabling decoupling of multi-conductor spatial magnetic fields and accurate sag estimation; their approach was validated through simulations and scale model tests. Lin et al. [19] developed an asymmetric dual-layer wireless sensor network for intelligent substations and, based on field measurements and WinProp simulations, provided guidance for node deployment in power IoT applications.

Table 1: Comparative summary of related studies.

| Study | Sensor Type | Target Fault Type | Performance Indicators | Energy Consumption | Limitations |
|---|---|---|---|---|---|
| Dadashizadeh Samakosh & Enayati [14] | Temperature sensor | Overload, thermal stress defects | Surface temperature, crimping pressure, and length | – | Focused solely on temperature variation; did not address multiple fault types |
| Chen et al. [15] | Sag measurement device | Sag variation | Efficiency improved by 28%; sag deviation of 1.96 % | – | Limited to sag monitoring; lacked multi-sensor coordination |
| Luo et al. [16] | FBG sensor | Sag, load | Prediction accuracy | – | Applicable only to localized deformation scenarios |
| Li et al. [17] | Optical fiber, MEMS, self-powered sensors | Overall line condition | – | – | Focused on sensor development; lacked specific application validation |

| | | | | | |
|---|---|---|---|---|---|
| Mai et al. [18] | Magnetic sensor | Overhead line | Simulation validation | – | Non-intrusive monitoring; lacked field testing |
| Lin et al. [19] | Wireless sensor network | Substation condition | Wireless coverage prediction, received power coverage | – | Targeted substations; not applicable to transmission lines |
| This study | Thermosensitive resonator, torque sensor, strain gauge | Strain clamp faults (cracking, deformation, bolt loosening) | Accuracy 94.8%; F1-score 94.4% | 12.8 mWh/day | Multi-sensor fusion, adaptable to diverse conditions, long-term stability, low power consumption |

Although previous studies have improved monitoring techniques and sensor design, several key limitations persist. Most existing approaches rely on single sensors or target only specific fault types, lacking multi-parameter sensing and fusion-based fault analysis. In addition, ultra-low-power operation and long-term online monitoring remain insufficient, resulting in high energy consumption and reduced device endurance in field applications. Furthermore, many studies are confined to laboratory environments, often employing scaled models or limited test scenarios, with inadequate field validation. To overcome these limitations, this study introduces an online monitoring approach for strain clamps that employs ultra-low-power, multi-sensor integration. The proposed system combines thermal, torque, and strain sensing units with an information fusion model to enable precise fault identification under diverse operating conditions. Both laboratory experiments and field trials on a 66 kV transmission line demonstrate the system's stability, accuracy, and energy efficiency, providing a practical solution for intelligent monitoring of transmission infrastructure.

# 3 Methods and system design

## 3.1 Overall system architecture

The online monitoring system for strain clamps in transmission lines was developed to achieve long-term real-time monitoring, accurate fault diagnosis, and intelligent management. It targets key operational parameters such as temperature, torque, deformation, and cracking, allowing for multi-source data fusion and dynamic operational analysis. The system adopts a hierarchical, modular design composed of three layers: the perception layer, the network layer, and the application layer. This architecture enables efficient bottom-up coordination across layers and maintains a closed-loop data flow for continuous monitoring and feedback, as illustrated in Figure 1.

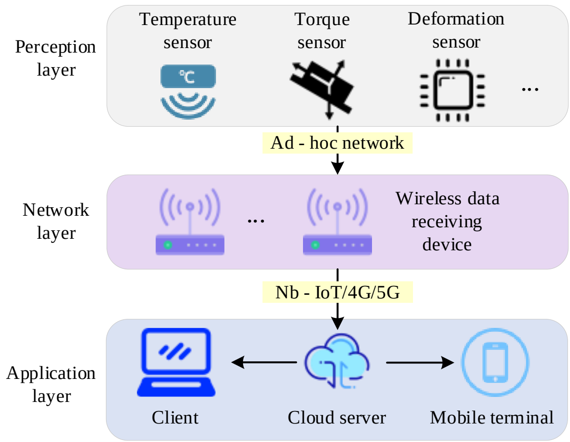


Figure 1: Overall system architecture.

At the perception layer, various ultra-low-power sensing nodes are deployed to monitor faults such as temperature rise, bolt loosening, and localized deformation during the operation of strain clamps. The sensors, manufactured using MEMS technology, provide high sensitivity, low power consumption, easy multi-point deployment, strong resistance to interference, and reliable long-term stability [20–22].

The network layer acts as the system's information transmission and processing hub. It collects data from the sensors and ensures consistent transmission and sharing among field devices. Through low-power wireless communication, multi-source data are quickly aggregated at the field level, processed at the edge, and transmitted to the server for further analysis. The application layer delivers data services and intelligent functions adapted to different operational requirements. By preprocessing and modeling the collected data, the system supports condition assessment, anomaly detection, and risk evaluation. With visualization interfaces and diagnostic algorithms, operators can monitor the operational status of strain clamps via centralized terminals, issue tiered alerts, and perform preventive maintenance on high-risk components.

Overall, the architecture prioritizes coordination among the perception, network, and application layers. By integrating ultra-low-power sensors, wireless communication, and intelligent diagnostics, it enables continuous online monitoring of strain clamps throughout their operational lifecycle.

## 3.2 Condition identification of transmission line strain clamps

Strain clamps on transmission lines are subjected to complex operating conditions, including temperature rise, bolt loosening, deformation, and cracking. Their safe operation is highly sensitive to variations in these parameters [23]. To enable high-precision, real-time monitoring, a multi-sensor information fusion approach is employed for condition identification. By integrating data from multiple sensor types, a multi-parameter profile of each clamp is constructed, providing a detailed representation of its operational state. The primary sensors used for monitoring are thermistors, strain gauges, and torque sensors. Thermistors measure temperature, strain gauges detect deformation, and torque sensors monitor bolt tightening status. Data from these sensors are combined through collaborative fusion to achieve accurate and reliable condition assessment.

Thermistor Sensor: Thermistors model temperature based on the resistance change of thermistor materials in response to temperature variations. They are typically classified as either Positive Temperature Coefficient (PTC) or Negative Temperature Coefficient (NTC), with resistance–temperature relationships described as:

$$R_{PTC}(T) = R_0 e^{\alpha(T-T_0)} \tag{1}$$
$$R_{NTC}(T) = R_0 e^{-\beta(T-T_0)} \tag{2}$$

where $R_0$ is the reference resistance, $\alpha$ and $\beta$ are material constants, and $T_0$ is the reference temperature. Through appropriate design of the thermistor resonator and reader antenna, the high sensitivity and low-loss characteristics of the thermistor are fully utilized, enabling monitoring of local temperature rise in strain clamps.

Strain Gauge Sensor: Strain gauges convert mechanical deformation of the clamp under wind, vibration, and thermal stress into measurable electrical signals. The basic relationship is:

$$\epsilon = \frac{\Delta R}{R} \cdot \frac{1}{k_s} \tag{3}$$

where $\epsilon$ is strain, $\Delta R$ is the change in gauge resistance, $R$ is the initial resistance, and $k_s$ is the gauge sensitivity coefficient.

Torque Sensor: Torque sensors measure torque changes during bolt tightening to assess bolt loosening. The instantaneous torque $M$ and rotation angle $\theta$ are related by:

$$M = k\theta \tag{4}$$

where $k$ is the calibration coefficient of the torque sensor.

Using these sensors, feature vectors reflecting the strain clamp condition are obtained as $x = [T, \epsilon, M]$, which serve as inputs for multi-sensor information fusion.

The data fusion process employs Dempster–Shafer (D–S) theory as the core algorithm for multi-sensor information integration. Compared with Bayesian inference and ensemble learning methods, D–S theory offers several advantages. Bayesian inference typically assumes that sensor data are independent, which may not hold in multi-sensor systems. This assumption can reduce performance, especially when sensor information is redundant or complementary. Ensemble learning methods can improve diagnostic accuracy but often require training multiple base models, which increases computational and storage overhead and is challenging to implement efficiently in low-power systems. In contrast, D–S theory does not rely on the independence assumption, effectively handling redundant and complementary information while providing a systematic framework for integrating uncertain data. This makes it highly adaptable and particularly accurate in scenarios with incomplete or uncertain sensor information. The overall workflow of the data fusion process is illustrated in Figure 2.

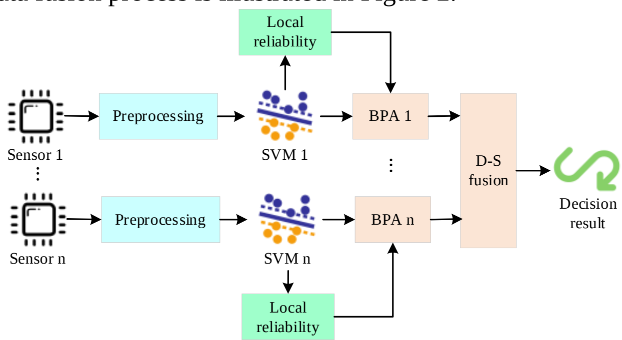


Figure 2: Intelligent Multi-Sensor Information Fusion Decision Flow.

In the multi-sensor fusion process, the objective is to obtain a consistent diagnostic result $D$ by integrating signals from different sensors. This is achieved by applying a fusion operator $F$ to the sensor signal set $S = \{s_1, s_2, \cdots, s_n\}$, producing a reliable decision:

$$D = F(S) \tag{5}$$

$F(*)$ represents the fusion operator, typically based on Dempster–Shafer (D–S) theory to handle uncertain information. D–S theory provides a systematic framework for evidence combination, effectively addressing ambiguity and uncertainty in multi-sensor data. Consider a hypothesis space $\Theta = \{\theta_1, \theta_2, \cdots, \theta_m\}$, where each sensor output is represented by a Basic Probability Assignment (BPA) $m_i$:

$$m_i: 2^\Theta \rightarrow [0,1], \sum_{A\subseteq\Theta} m_i(A) = 1 \quad (6)$$

For multiple independent sensor evidences, the Dempster rule is applied to combine them. Let $m_1$ and $m_2$ be BPAs from two independent evidence sources. Their combination $m(A)$ is given by:

$$m(A) = \frac{1}{1-K} \sum_{B\cap C=A} m_1(B) m_2(C) \quad (7)$$

where $K$ is the conflict coefficient used to adjust for contradictory evidence:

$$K = \sum_{B\cap C=\phi} m_1(B) m_2(C) \quad (8)$$

Through iterative combination, multiple sensor evidences can be fused into a consistent judgment $m_{fused}$, enabling evaluation of conditions such as clamp cracking, deformation, and bolt loosening. To further enhance diagnostic precision, belief functions are introduced to calculate the lower $Bel(A)$ and upper bounds of credibility $Pl(A)$:

$$Bel(A) = \sum_{B\subseteq A} m(B) \quad (9)$$

$$Pl(A) = \sum_{B\cap A\neq\phi} m(B) \quad (10)$$

These calculations provide an interval-based representation of uncertainty, supporting more reliable fault diagnosis.

To illustrate the application of D–S theory in multi-sensor data fusion, consider three sensors measuring different physical quantities—strain, temperature, and vibration—to detect a clamp cracking fault. Each sensor output corresponds to a BPA representing the sensor's confidence in different hypotheses. Assume the fault hypothesis space is $\Theta = \{\theta_1, \theta_2\}$, where $\theta_1$ indicates "clamp cracking" and $\theta_2$ indicates "no fault." The sensor outputs are $m_1$, $m_2$, and $m_3$. First, $m_1$ and $m_2$ are combined using the Dempster rule. The conflict coefficient is calculated as:

$$K = m_1(\{\theta_1\}) \cdot m_2(\{\theta_2\}) + m_1(\{\theta_2\}) \cdot m_2(\{\theta_1\}) \quad (11)$$

The fused BPA values are then computed:

$$m_{12}(\{\theta_1\}) = \frac{1}{1-K}(m_1(\{\theta_1\}) \cdot m_2(\{\theta_1\}) + m_1(\{\theta_2\}) \cdot m_2(\{\theta_2\}) \quad (12)$$

$$m_{12}(\{\theta_2\}) = \frac{1}{1-K}(m_1(\{\theta_1\}) \cdot m_2(\{\theta_2\}) + m_1(\{\theta_2\}) \cdot m_2(\{\theta_1\}) \quad (13)$$

$m_{12}$ is combined with $m_3$ using the same procedure. The final fusion result, $m_f(\{\theta_1\})$ and $m_f(\{\theta_2\})$, represents the system's ultimate diagnostic output. The relative magnitudes of $m_f(\{\theta_1\})$ and $m_f(\{\theta_2\})$ indicate the confidence in "clamp cracking" versus "no fault." The pseudocode for the D–S theory-based multi-sensor fusion model is shown in Figure 3.

```
# Step 1: Collect data from all sensors
for each sensor in S:
    data[sensor] = collect_data(sensor)  # Collect sensor data (temperature, strain, torque)
    BPA[sensor] = calculate_BPA(data[sensor])  # Calculate BPA for each sensor

# Step 2: Fuse the sensor data using Dempster's Rule
fused_BPA = BPA[1]  # Start with the first sensor's BPA
for i = 2 to number_of_sensors:
    conflict_coefficient = calculate_conflict(BPA[fused_BPA], BPA[i])
    fused_BPA = combine_BPA(fused_BPA, BPA[i], conflict_coefficient)

# Step 3: Compute belief and plausibility for the fused result
belief = compute_belief(fused_BPA)
plausibility = compute_plausibility(fused_BPA)

# Step 4: Make decision based on belief and plausibility
if belief['crack'] > threshold:
    decision = "Crack detected"
else if plausibility['no_fault'] > threshold:
    decision = "No fault detected"
else:
    decision = "Indeterminate"

return decision  # Final decision

# Helper functions:
function collect_data(sensor):
    return read_sensor(sensor)  # Read data from the sensor

function calculate_BPA(data):
    return apply_sensor_model(data)  # Calculate BPA for each sensor's data

function calculate_conflict(BPA1, BPA2):
    return sum(BPA1[A] * BPA2[B] for A, B in conflict_sets)  # Conflict coefficient

function combine_BPA(BPA1, BPA2, conflict_coefficient):
    return normalize(BPA1 * BPA2 / (1 - conflict_coefficient))  # Combine BPAs using Dempster's rule

function compute_belief(BPA):
    return sum(BPA[A] for A in hypothesis_subsets)  # Compute belief

function compute_plausibility(BPA):
    return sum(BPA[A] for A in hypothesis_plausible_sets)  # Compute plausibility
```

Figure 3: Pseudocode of the D–S theory-based multi-sensor data fusion model.

The collaborative management, fault diagnosis, information judgment, reasoning, fusion, and perception learning units together constitute the core components of the multi-sensor collaborative perception system (Figure 4).

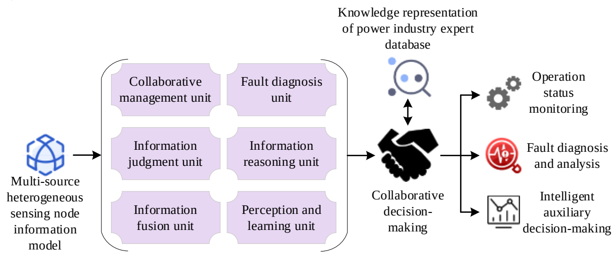


Figure 4: Main units of the multi-sensor multi-parameter collaborative perception model.

The collaborative management unit handles task requests from the perception layer and communications with other units, scheduling tasks and coordinating information flow to ensure spatiotemporal synchronization across all sources. The fault diagnosis unit processes diagnostic and feedback data from input/output units, completing a closed-loop diagnostic cycle. The information judgment and reasoning units combine historical data with a Bayesian inference model to perform probabilistic analyses for decision-making. The information fusion unit integrates multi-sensor data using Dempster–Shafer evidence theory. The perception learning unit updates prior probabilities based on historical statistics and fault records, enabling adaptive condition assessment. The overall system architecture can be represented as:

$$y_{t+1} = G(y_t, x_t, m_{fused}) \tag{14}$$

where $y_t$ denotes the system condition at time $t$, $x_t$ is the sensor feature vector, and $G(*)$ is the multi-unit collaborative fusion function.

The intelligent sensing unit is implemented on a System-on-Chip (SoC) platform, with functional modules built using Intellectual Property (IP) cores to integrate sensing, computation, communication, and power management. By combining a microprocessor with a Field-Programmable Gate Array (FPGA), the system enables real-time perception, feature extraction, and information fusion reasoning under operational conditions. Its primary function can be expressed as:

$$y_t = f_{SOC}(x_t, p_t) \tag{15}$$

where $p_t$ is the SoC internal configuration vector, including sampling frequency, communication power, and processing strategy.

## 3.3 Design of ultra-low-power sensing devices

Strain clamps in transmission lines operate continuously under high voltage, strong electromagnetic interference, and harsh environmental conditions. These factors place strict demands on online monitoring devices, including miniaturization, low power consumption, high reliability, and long-term energy supply. The design strategy emphasizes developing perception units capable of stable operation under extreme conditions while meeting engineering requirements for size, power efficiency, and service life. Table 2 summarizes the key technologies and implementation methods for the ultra-low-power sensing devices.

Table 2: Key technologies and implementation methods.

| Key Technology | Implementation and Description | Applicable Sensor Type |
|---|---|---|
| Sensor Miniaturization | Based on MEMS technology; integration at millimeter/micron scale using photolithography, etching, thin-film deposition, and ultra-precision machining; multiple physical effects sensed within a single module. | Thermistor resonator, strain gauge, torque sensor |
| Long-Term Reliability and Lifespan | Industrial-grade components, derating design, redundancy, heat resistance optimization; packaging provides electrical insulation, prevention of corona discharge, and EMI robustness; modular design supports online replacement and periodic calibration; software enhances configuration quality. | All sensor modules |
| Ultra-Low-Power Management | Work mode switching (sleep/wake), including full wake, random wake, predictive-assisted wake, or task-cycle wake modes; dynamic adjustment of data acquisition and transmission frequency balances energy consumption and monitoring precision. | Thermistor resonator, strain gauge, torque sensor |
| Modular Energy Supply and Wireless Recharging | Integration of micro-batteries, supercapacitors, and environmental energy harvesting; wireless power transfer via electromagnetic induction, strongly coupled resonant electromagnetic, ultrasonic, or | Micro-battery, supercapacitor, wireless energy receiver module |

| | | |
|---|---|---|
| | microwave methods; coupling of online harvesting with fixed-terminal charging achieves continuous supply and energy scheduling. | |
| Environmental Adaptability | Optimized for high-voltage electromagnetic conditions, temperature fluctuations, and mechanical vibration to ensure stable data acquisition under extreme conditions; topological optimization balances transmission efficiency, safety, and spatial coupling. | All sensor modules |

Sensor miniaturization leverages MEMS technology and integrates photolithography, etching, thin-film deposition, and ultra-precision machining to enable multi-physical sensing—including temperature, strain, and torque—within a single module. This approach significantly reduces device size and power consumption while enhancing environmental adaptability and manufacturing consistency. Long-term stability is ensured through the use of industrial-grade components, redundant designs, modular packaging, and online calibration, along with replaceable power modules. Ultra-low-power operation is achieved via sleep/wake mode switching and dynamic adjustment of monitoring frequency, effectively balancing energy consumption and measurement accuracy. The energy supply combines micro-batteries and supercapacitors with environmental energy harvesting and wireless replenishment. An energy scheduling algorithm manages charge and discharge across storage elements, ensuring continuous operation even under extreme conditions. The specifications for each sensor are listed in Table 3.

Table 3: Sensor specifications and calibration details.

| Sensor Type | Model | Sampling Rate | Measurement Range | Sensitivity | Accuracy | Calibration Method |
|---|---|---|---|---|---|---|
| Strain Gauge | BHB120-3CA250 | 1 Hz – 1 kHz | 3-axis strain, ±2500 με | Sensitivity coefficient: 1.79 | ±0.5 % FS | Multi-point calibration using a calibration rig |
| Torque Sensor | Kistler 4527C | 1 Hz – 10 kHz | ±500 Nm | 2.0 mV/V/Nm | ±0.3 % FS | Calibrated with standard loads |
| Thermistor Resonator | Microchip TC1047 | 0.1 Hz – 100 Hz | –40 °C to 125 ° C | 20 mV/°C | ±0.3 ° C | Calibrated in controlled environmental temperature |
| Deformation Sensor | FOS-11 | 1 Hz – 1 kHz | ±10 mm | 0.2 mV/mm | ±0.2 % FS | Calibrated using standard deformation values |

The wireless power transfer system is shown in Figure 5. Depending on the application scenario, electromagnetic induction, strongly coupled resonance, ultrasonic, or microwave techniques may be employed, each providing specific advantages in efficiency, coupling, and safety. Topological optimization is used to achieve an efficient spatial layout and energy transmission, supporting the long-term online monitoring of strain clamps.

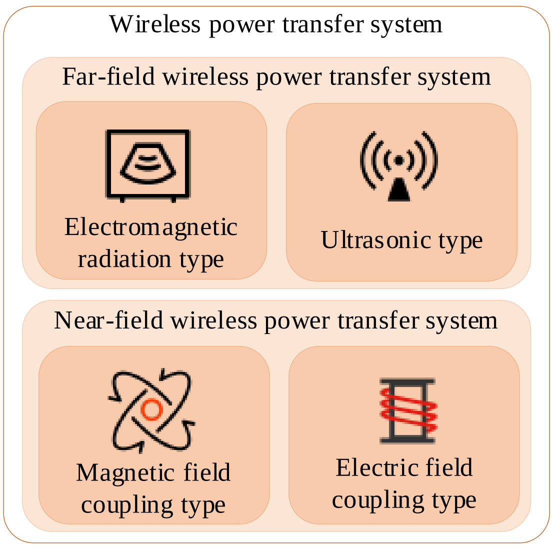


Figure 5: Wireless power transfer system.

### 3.4 Online monitoring software system and diagnostic platform implementation

The operating conditions of transmission line strain clamps are complex and variable, and hardware sensors alone cannot provide full lifecycle health management. Therefore, software and the diagnostic platform form the other two pillars of the system architecture. The design strategy integrates perception with intelligent diagnostics, enabling high-volume data reception, situational awareness, and decision support in the cloud. This approach establishes a platform comprising monitoring, analysis, evaluation, and early-warning modules.

Following development, the devices were installed and commissioned on a 66 kV transmission line. Sensor data were transmitted through gateways to the cloud, providing real-time measurements of temperature, strain, deformation, and torque under varying operating conditions. The first module, the Situational Awareness Module, visually displays key operational parameters and issues warnings or alerts when thresholds are exceeded. This enables maintenance personnel to quickly identify anomalies and carry out condition-based or preventive maintenance. Beyond visualization, the module also supports on-site verification, ensuring that monitoring results align with manual inspections and flaw-detection instruments.

The second key module is the multi-sensor, multi-parameter diagnostic module. This module stores data collected from various sensors in a database and performs real-time condition diagnosis of the strain clamps using a collaborative perception model. It employs an event-driven fault diagnosis approach, where the diagnostic process is triggered only when sensor measurements exceed predefined thresholds. The specific thresholds are as follows: a temperature threshold, where a warning is issued if the clamp temperature exceeds 85 °C and an alarm is triggered if it exceeds 100 °C; a strain threshold, with a warning at 1.2 times the normal value and an alarm at 1.5 times; a deformation threshold, with a warning at 2% above the standard value and an alarm at 3%; and a torque threshold, with a warning at 10% above the design load and an alarm at 15%. The system also calculates probability scores for fault occurrence using multi-sensor data fusion. Based on the fused sensor data, the probability of each fault hypothesis is computed. If a fault probability exceeds 70%, a warning is issued; if it exceeds 90%, an alarm is triggered. These confidence thresholds are determined from historical data and expert knowledge and can be dynamically adjusted according to the operational context. By integrating information from multiple sensors, the system does not rely solely on single-parameter thresholds but evaluates the overall condition, significantly improving diagnostic accuracy and reliability. The module is capable of outputting the operational status levels of strain clamps and generating dynamic diagnostic reports. On-site diagnostic results are cross-validated with sensor measurements, forming a positive feedback loop that continuously refines and optimizes the model.

The third module, the Query and Statistics Module, enables archival, retrieval, and multi-dimensional analysis of historical data. Operators can monitor the condition trajectories of strain clamps over time, detect long-term trends, and identify potential risks. By integrating sensing and computation, the software system and diagnostic platform overcome the limitations of traditional isolated monitoring systems, creating an ecosystem that combines data acquisition, real-time analysis, intelligent diagnostics, and traceable management.

## 4 Experiments and result analysis

### 4.1 Laboratory performance testing and validation

The diagnostic performance of the ultra-low-power sensing devices and the multi-sensor information fusion model was first validated offline under controlled laboratory conditions. Calibration and performance tests were systematically conducted for thermistor resonators, torque sensors, and strain gauges, allowing precise measurement of temperature, resistance, torque, and strain signals. Sensor data were collected under various simulated operating conditions, including temperature fluctuations, mechanical stress, and bolt loosening scenarios. These data were used to establish single-sensor diagnostic models as well as a multi-sensor information fusion model, with the goal of evaluating the models' ability to accurately detect typical strain clamp faults.

Data were collected from seven test points. At each point, every sensor continuously recorded measurement for one hour, with a data point logged every second. Consequently, one day of sensor data consisted of second-level measurements, and over a total of seven days, 25,200 test cases were obtained. Single-sensor models were developed independently for each sensor type using a Support Vector Machine (SVM) classifier. Performance metrics, including accuracy, precision, and F1-score, were rigorously evaluated using 5-fold cross-validation. In contrast, the multi-sensor information fusion model combined signals from all sensors within an ensemble classification framework. Fault diagnosis employed a weighted voting strategy, while a decision tree algorithm performed classification, enabling the model to exploit complementary information from multiple sensors and improve reliability. The diagnostic results, comparing single-sensor models with the multi-sensor fusion model, are presented in Figure 6, highlighting the performance gains achieved through multi-source information integration.

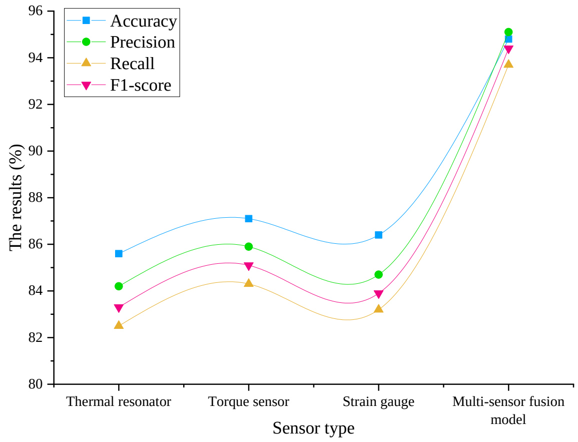


Figure 6: Comparison of diagnostic performance between single-sensor and fusion models.

The results in Figure 6 demonstrate that the multi-sensor fusion model significantly outperforms the single-sensor models. The fusion model achieved an accuracy of 94.8% and an F1-score of 94.4%, both exceeding the performance of any individual sensor. Compared to the best-performing single sensor, the torque sensor, the fusion model improved accuracy and F1-score by 8.84% and 10.9%, respectively. These findings indicate that multi-source information fusion substantially enhances the identification of strain clamp faults, including cracking, deformation, and bolt loosening, providing a reliable basis for field condition monitoring. To assess energy efficiency, the power consumption of each sensor and the fusion model was measured, as shown in Figure 7. All energy consumption values represent the average of five experimental runs, with standard deviations calculated to reflect data variability.

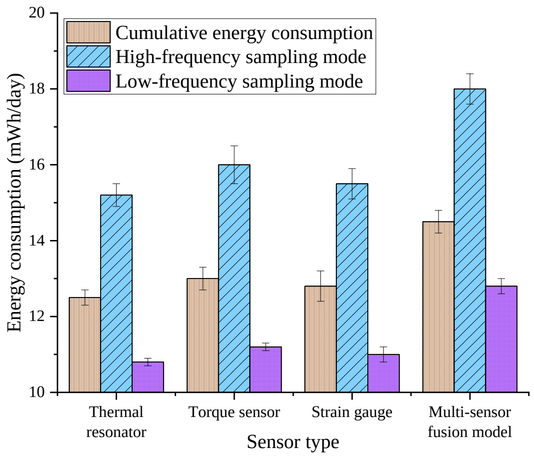


Figure 7: Comparison of cumulative energy consumption.

As shown in Figure 7, under standard operating conditions, the fusion model consumes 14.5 mWh per day, slightly higher than the 12.5–13.0 mWh recorded for individual sensors. In high-frequency sampling mode, energy consumption of the multi-sensor fusion model increases to 18.0 mWh/day, approximately 3–5 mWh higher than under standard operation. Conversely, in low-frequency sampling mode, consumption decreases to 12.8 mWh/day, approaching the levels observed for single-sensor operation. These results indicate that energy consumption is strongly influenced by both sampling frequency and operating mode. By selecting an appropriate sampling strategy, an optimal balance can be achieved between energy efficiency and diagnostic performance. This approach ensures long-term sustainability of the monitoring system and extends the operational lifetime of the sensors, providing a practical and effective solution for continuous online monitoring of strain clamps over extended periods.

To comprehensively evaluate system performance, the proposed multi-sensor fusion model was compared with classical adaptive control methods, including adaptive backstepping control, neural adaptive control, observer-based control, as well as other mainstream approaches such as Convolutional Neural Network–Long Short-Term Memory (CNN-LSTM). The results are summarized in Table 4.

Table 4: Comparison with other methods.

| Method | Accuracy (%) | F1-score (%) | Detection Time (s) | Energy Consumption (mWh/day, mean ± SD) | CPU Usage (%) | Memory (MB) |
|---|---|---|---|---|---|---|
| Multi-sensor fusion model | 94.8 | 94.4 | 0.35 | 14.5 ± 0.3 | 45.2 | 147 |
| Adaptive backstepping control | 91.5 | 92.0 | 0.58 | 18.2 ± 0.4 | 52.1 | 158 |
| Neural adaptive control | 92.5 | 93.0 | 0.65 | 18.5 ± 0.3 | 54.7 | 163 |
| Observer-based control | 90.8 | 91.5 | 0.55 | 17.8 ± 0.3 | 48.6 | 151 |
| Single-sensor SVM model | 86.5 | 85.7 | 0.42 | 12.5 ± 0.2 | 38.4 | 126 |
| Random Forest fusion model | 91.2 | 90.5 | 0.48 | 17.6 ± 0.3 | 50.3 | 139 |
| CNN-LSTM hybrid model | 92.8 | 92.1 | 0.62 | 19.4 ± 0.5 | 62.5 | 182 |

| | | | | | | |
|---|---|---|---|---|---|---|
| Autoencoder fault detection model | 90.7 | 89.8 | 0.57 | 16.9 ± 0.4 | 55.0 | 171 |

Table 4 shows that the multi-sensor fusion model outperforms other control and deep learning methods in terms of accuracy and F1-score, while achieving faster response times and lower energy consumption. Compared with the CNN-LSTM model, the fusion model reduces energy consumption by 25.3% and shortens response time by 43.5%, with a CPU usage of 45.2% and memory footprint of 147 MB. These advantages stem from several factors: the model fuses thermal, torque, and strain signals through a weighted decision framework, enhancing feature complementarity and robustness; a predictive-assisted wake-up mechanism minimizes energy waste from high-frequency sampling by enabling active monitoring during critical periods and low-power standby during stable operation; and dynamic feature weighting adjusts sensor contributions according to operating conditions, improving detection accuracy. The system's low energy consumption further supports long-term monitoring and efficient resource management, making it suitable for practical online applications. However, under extreme conditions such as low temperatures, high humidity, or strong electromagnetic interference, sensor drift or feature distortion may occur, potentially blurring classification boundaries. Future work may include temperature–humidity compensation algorithms or fuzzy adaptive control strategies for online model adjustment. Lightweight deep fusion architectures, such as Tiny-CNN or edge-based autoencoder fusion, could also be explored to further reduce energy consumption and enhance generalization.

The diagnostic performance of the multi-sensor fusion model for typical faults—including bolt loosening, clamp cracking, fitting deformation, and local overheating—was further analyzed, as shown in Table 5.

Table 5: Diagnostic performance by fault type.

| Fault Type | Accuracy (%) | Precision (%) | Recall (%) | F1-score (%) |
|---|---|---|---|---|
| Bolt loosening | 95.3 | 96.7 | 95.0 | 95.8 |
| Clamp cracking | 94.6 | 95.2 | 93.8 | 94.5 |
| Fitting deformation | 94.4 | 94.0 | 92.0 | 93.0 |
| Local overheating | 94.7 | 94.4 | 94.1 | 94.2 |
| Average | 94.8 | 95.1 | 93.7 | 94.4 |

Table 5 indicates that the multi-sensor fusion model maintains high diagnostic performance across different fault types, with overall accuracy exceeding 94%. Bolt loosening and clamp cracking show the highest F1-scores (95.8% and 94.5%, respectively), demonstrating that the fused multi-parameter features effectively capture mechanical and thermal variations. Detection performance for fitting deformation and local overheating is slightly lower due to partial signal overlap in early stages of these faults. Overall, the multi-parameter fusion strategy enhances robustness and diagnostic accuracy for multiple fault types, providing reliable support for on-site status assessment and early warning.

To verify the advantages of Dempster–Shafer (D-S) theory, benchmark tests were conducted comparing Bayesian inference, weighted averaging fusion, and Extreme Gradient Boosting (XGBoost), with results summarized in Table 6.

Table 6: Comparison of different fusion methods.

| Method | Accuracy (%) | F1-score (%) | Detection Time (s) | Energy Consumption (mWh/day, mean ± SD) |
|---|---|---|---|---|
| D-S Theory | 94.8 | 94.4 | 0.35 | 14.5 ± 0.3 |
| Bayesian Inference | 92.3 | 90.6 | 0.23 | 15.2 ± 0.3 |
| Weighted Average Fusion | 92.0 | 90.2 | 0.20 | 15.0 ± 0.2 |
| XGBoost | 93.0 | 91.7 | 0.38 | 18.1 ± 0.5 |

As shown in Table 6, the multi-sensor fusion model based on D-S theory outperforms the other fusion methods. It achieves the highest accuracy and F1-score, clearly exceeding the performance of Bayesian inference, weighted averaging, and XGBoost. Although Bayesian inference and weighted averaging offer slightly faster detection times, their diagnostic accuracy is lower. Compared with XGBoost, the D-S model achieves slightly shorter detection times (0.35 s vs. 0.38 s) while consuming less energy, highlighting its suitability for low-power platforms. Overall, the D-S-based multi-sensor fusion model provides higher fault detection precision with lower energy consumption, making it an effective solution for long-term online monitoring in energy-constrained environments.

## 4.2 Field pilot application and performance evaluation

A pilot monitoring study was conducted on a 66 kV transmission line operated by the State Grid Siping Power Supply Company to evaluate the multi-sensor fusion model in detecting strain clamp faults, including cracking, deformation, and bolt loosening. To ensure safe operation under high-voltage conditions, all sensors and acquisition devices were designed with high-voltage isolation. Electrical isolation was further enhanced using insulating materials and shielding, while electromagnetic interference filters were installed at critical line interfaces to minimize signal disturbance. The hardware design complied with relevant State Grid and International Electrotechnical Commission (IEC) high-voltage safety standards, and internal testing confirmed insulation, voltage withstand, and anti-interference performance, ensuring personnel and equipment safety under 66 kV operating conditions. Under these safety measures, the system's diagnostic accuracy, micro-power management strategy, and energy scheduling scheme were evaluated to verify the extension of system operational life. During field deployment, 30 strain clamps were equipped with thermistor resonators, torque sensors, and strain gauges to continuously collect real-time data under varying environmental and mechanical conditions. The multi-sensor fusion model processed these multi-source signals to identify faults and generate diagnostic reports, which were then validated against manual inspection results. In addition to fault detection, system stability, response performance, and energy consumption were monitored to comprehensively assess the monitoring solution. Figure 7 presents the confusion matrix for strain clamp fault diagnosis, illustrating the model's performance across different fault types and operating conditions.

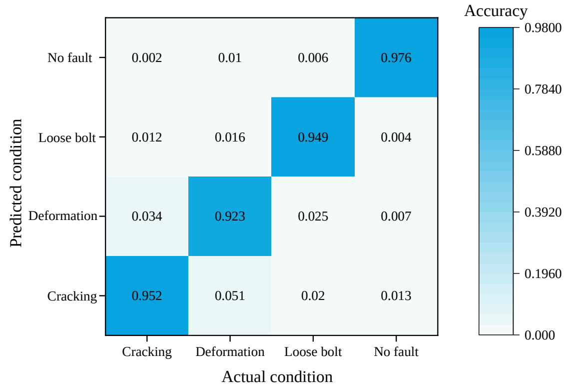


Figure 8: Confusion matrix of strain clamp fault diagnosis.

As shown in Figure 8, the model maintains consistently high diagnostic accuracy across different fault types. Cracks and fault-free conditions were detected with over 95% accuracy, demonstrating the system's ability to reliably distinguish between healthy and compromised clamps. For deformation and bolt loosening, accuracy remained high at 92.3% and 94.9%, respectively, indicating that the multi-sensor fusion approach effectively captures subtle mechanical and structural changes. Overall, the system demonstrates high fault-detection accuracy. Although occasional misclassifications occur, the errors are minor, indicating that the system can effectively distinguish between different fault types in practical applications. Moreover, the confusion matrix reflects classification performance and directly informs the system's maintenance decision logic. The system implements a three-tiered response mechanism based on diagnostic results: 1. Level 1 Warning (Minor Anomaly): If the model's confidence is low or adjacent classes are detected (e.g., "bolt loosening" misclassified as "local overheating"), the system flags a potential risk without triggering immediate maintenance. The monitoring platform increases observation frequency to track the situation. 2. Level 2 Warning (Moderate Anomaly): When the same fault type is detected repeatedly, or the confusion matrix indicates a high probability of adjacent fault transitions (e.g., between "deformation" and "loosening"), the system triggers a manual inspection task. 3. Level 3 Alarm (Severe Anomaly): If the identification is stable with high confidence (≥95%) and corresponds to critical faults such as "clamp cracking" or "severe overheating," the system automatically reports to the grid operations center and recommends power shutdown for maintenance. This tiered decision-making approach, grounded in the probabilistic distribution of the confusion matrix, enables intelligent responses according to fault severity. It prevents unnecessary maintenance while ensuring timely intervention for potential hazards, thereby improving safety and operational efficiency.

To enhance energy efficiency in the multi-sensor fusion model, four wake-up strategies are employed: full wake-up, random wake-up, predictive-assisted wake-up, and task-cycle wake-up. The predictive-assisted wake-up strategy relies on historical trend prediction to determine the optimal next wake-up time, avoiding unnecessary frequent activations. Specifically, the mechanism uses historical sensor data and machine learning–based time series models, such as LSTM, to forecast potential events or state changes in the upcoming period, optimizing wake-up timing. In this approach, each sensor node independently predicts and decides when to wake, based on its local historical data, rather than relying on a centralized controller. Each node determines whether to enter low-power mode or wake based on its own data and predictions. This decentralized strategy reduces communication overhead and further optimizes energy consumption. Five experiments were conducted, and the average system endurance, response time, and energy consumption under the four wake-up strategies are presented in Figure 9.

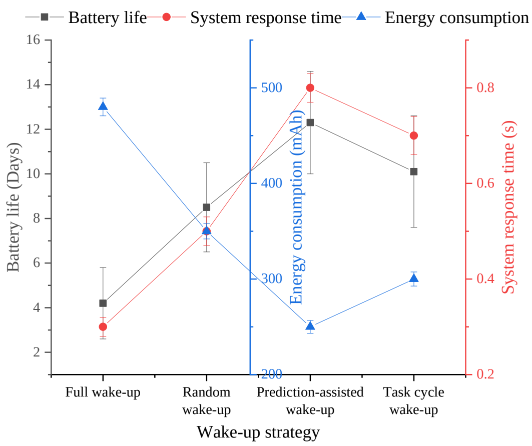


Figure 9: Comparison of endurance under different wake-up strategies.

Figure 9 shows that the predictive-assisted wake strategy achieves the longest system endurance of 12.3 days with relatively low energy consumption of 250 mAh, though the response time is slightly longer at 0.8 s. The task-cycle wake strategy consumes slightly more energy than predictive-assisted wake while still maintaining relatively long endurance. In contrast, the full wake strategy exhibits the shortest endurance at 4.2 days and the highest energy consumption of 480 mAh, but offers the fastest response time of 0.3 s. Overall, the predictive-assisted wake strategy provides an effective balance between endurance and energy efficiency, making it well suited for long-term online monitoring applications.

## 4.3 Discussion

In this study, the proposed multi-sensor fusion-based online monitoring system, combined with a predictive-assisted wake strategy, demonstrated high diagnostic accuracy and energy efficiency. Compared with existing approaches, the proposed method shows advantages in detection precision, energy consumption, and response speed. Boulkroune et al. proposed an output-feedback projection lag synchronization scheme for chaotic drive–response systems with input dead zones and sector nonlinearities. The method employs a variable-structure controller and an adaptive fuzzy system to handle uncertain dynamics [24]. This method primarily addresses challenges in unmeasurable system states and dynamic uncertainties, focusing on system stability and synchronization, but it does not specifically target fault diagnosis in physical devices such as strain clamps. In contrast, the monitoring system presented here achieves high fault detection accuracy, with an overall accuracy of 94.8% and an F1-score of 94.4%. By integrating data from multiple sensors, it effectively enhances diagnostic performance in complex environments through the synergistic use of temperature, strain, and torque information. Boulkroune et al. also introduced a nonsingular fixed-time sliding mode-based adaptive fuzzy controller for fixed-time synchronization of heterogeneous fractional-order chaotic systems [25]. While this approach demonstrates good convergence in nonlinear systems, it lacks focus on energy efficiency and does not directly address device-level fault diagnosis. By comparison, the method ensures high diagnostic accuracy and emphasizes energy efficiency, using optimized sampling strategies such as predictive-assisted wake to reduce power consumption without compromising diagnostic performance. This makes it well suited for long-term, energy-constrained online monitoring applications. Zouari et al. proposed a Lyapunov-based robust adaptive backstepping control method for uncertain single-input single-output nonlinear systems, emphasizing stability and convergence of tracking errors [26]. Although theoretically capable of ensuring error convergence, such methods may encounter practical limitations in complex electrical system fault diagnosis due to high model complexity and energy demands. In contrast, the proposed system leverages multi-sensor fusion and simplified classification models to achieve high diagnostic accuracy while maintaining low energy consumption, meeting the requirements of extended online monitoring. Zouari et al. further developed robust neural adaptive and indirect neural adaptive control strategies for multivariable uncertain nonlinear systems [27]. While robust and effective at disturbance rejection, these approaches incur significant computational overhead, resulting in lower energy efficiency. The multi-sensor fusion system presented here employs low-power sensors combined with an effective energy management strategy, enabling high-accuracy diagnosis while minimizing energy consumption, particularly during low-power operation. Rigatos et al. introduced a nonlinear optimal control method for gas centrifugal compressors, using linearized models and feedback controllers to handle uncertainties and external disturbances [28]. Although computationally efficient, this approach is complex and not optimized for the energy requirements of long-term online monitoring. By contrast, the multi-sensor fusion model developed in this study maintains high accuracy while using adaptive sampling and predictive-assisted wake strategies to significantly reduce long-term energy consumption, making it suitable for real-time monitoring and fault warning in smart grids. Merazka et al. proposed a fuzzy adaptive output-feedback control approach, employing high-gain observers to estimate unmeasurable states and fuzzy systems to model uncertainties for closed-loop stability [29]. While robust and stable, this method has relatively low energy efficiency and focuses on state estimation in complex systems rather than direct fault diagnosis of physical devices. The online monitoring system proposed here integrates multiple sensors and fusion algorithms to directly address the specific fault types of strain clamps, achieving more efficient and accurate online fault detection while maintaining low power consumption. Overall, compared with the aforementioned studies, the multi-sensor fusion-based online monitoring technology presented in this work offers clear advantages in accuracy, response speed, and energy efficiency. By integrating diverse sensor data and advanced energy management strategies, the system ensures high-performance diagnosis while effectively controlling energy consumption, making it highly suitable for real-time monitoring and fault warning in complex smart grid environments.

Although the proposed online monitoring system demonstrates high accuracy and low energy consumption under normal conditions, its performance may be affected under extreme environmental conditions. For example, in low-temperature, high-humidity, or high-wind environments, sensor accuracy may be compromised. Thermistor resonators and strain gauges are particularly sensitive to temperature and humidity variations. Under extreme temperatures, thermal elements may drift, leading to inaccurate measurements, while high humidity can affect the resistance of strain gauges, reducing the reliability of fault diagnosis. In such harsh conditions, the system may require additional sensor redundancy or more frequent wake cycles to maintain stability, which inevitably increases energy consumption. For instance, under low-temperature conditions, ensuring continuous monitoring may necessitate higher-frequency wake-ups to detect sudden faults, consuming extra power. Therefore, improving the system’s robustness against environmental influences and minimizing their impact on performance is a key direction for future research. This could be achieved through temperature compensation, humidity correction algorithms, and dynamic adjustment of fault-diagnosis models.

Different transmission line types—high-, medium-, and low-voltage—as well as geographic variations, may also affect system performance. High-voltage and low-voltage lines differ significantly in load fluctuations, fault modes, and environmental conditions, requiring the system to dynamically adapt to specific line characteristics. In mountainous areas, regions with high electricity demand, or coastal environments, the system must accommodate complex conditions, such as frequent weather changes and larger load variations. In these scenarios, adaptive operation can be achieved through flexible sensor fusion and predictive wake strategies. Specifically, an environmental-awareness module can automatically adjust monitoring frequency and wake strategies based on real-time data, ensuring efficient operation and accurate fault diagnosis under diverse conditions. To further enhance long-term stability and operational efficiency, future developments could integrate adaptive control methods, such as fuzzy control or nonlinear optimal control, enabling real-time tuning of system parameters to optimize monitoring and energy management, thereby improving both energy efficiency and diagnostic accuracy.

Regarding system scalability, when monitoring hundreds or even thousands of strain clamps, bandwidth requirements and server loads become critical. As the number of sensors increases, the system must handle large volumes of real-time data, potentially creating transmission bottlenecks and limiting server processing capacity. For large-scale deployment, data acquisition, transmission, and processing workflows need to be optimized. Edge computing can be employed to offload data processing tasks to local nodes, reducing the burden on central servers. Data compression and distributed storage can further enhance scalability. To maintain diagnostic accuracy at scale, the system should support efficient parallel computation and robust fault-tolerant mechanisms, ensuring reliable results even when multiple nodes process data simultaneously.

The proposed online monitoring system improves fault diagnosis accuracy for transmission lines but also has broad practical applications, particularly in predictive maintenance for smart grids. By continuously monitoring the health of strain clamps, the system can identify potential faults in advance and estimate maintenance intervals, enabling necessary interventions without interrupting grid operation. This approach reduces equipment failure rates, lowers maintenance costs, and enhances grid reliability and stability. In smart grid applications, the system can integrate with existing dispatch and monitoring platforms, sharing data and leveraging fault predictions to optimize grid operation, minimize downtime, and enhance overall grid intelligence.

# 5 Conclusion

This study proposed an ultra-low-power online monitoring approach for transmission line strain clamps, employing multi-sensor collaborative perception and a fusion model to detect clamp faults. Validation results showed that the fusion model significantly outperformed single-sensor methods, demonstrating that integrating multi-source information effectively enhances fault diagnosis capability. These findings provide reliable technical support for field monitoring and contribute to improving the operation and maintenance of transmission lines. Furthermore, by comparing energy consumption and operational endurance under different wake-up strategies, the predictive-assisted wake strategy was shown to extend system endurance while reducing energy use, offering practical guidance for selecting wake-up strategies in energy-constrained applications.

Although the proposed method can detect major fault types under different wake-up strategies, it has certain limitations in monitoring high-frequency or transient faults. For example, some faults, such as arc flashovers or instantaneous short circuits, may occur and conclude during wake-up delays, making timely detection impossible. With a system response time of 0.8 s, these rapid faults could go undetected, potentially leading to misdiagnosis or missed events. This limitation may affect diagnostic accuracy and, consequently, the reliability of maintenance decisions during sudden, fast-changing fault conditions. Future research could focus on improving the system's wake-up mechanism and fault detection algorithms, particularly for applications requiring higher response speed. By optimizing system architecture and exploring more efficient wake-up strategies and real-time detection algorithms, the ability to capture high-frequency faults could be significantly enhanced. In parallel, more precise energy management strategies could help extend operational endurance without compromising responsiveness, meeting the monitoring needs of transmission lines under complex conditions. Moreover, the proposed approach is not limited to transmission line monitoring; it could be extended to other power facilities, transportation systems, and similar applications, providing technical support for the construction and maintenance of intelligent infrastructure.

# References

[1] Chen J, Xu H, Liu L, et al. Defect Detection Technology of Tension Clamps Based on UAV. GBP Proceedings Series, 2025, 7, pp. 46-50.

[2] Shao H, Lv J, Wang J, et al. Automatic crimping state classification in X-ray images of crimped tension clamp. Nondestructive Testing and Evaluation, 2025, 40(2), pp. 610-626.

[3] Cloostermans B, Pronk D, Bruckenburg B, et al. Bolted Flange Connection Leakage: a Systematic Review of Monitoring Challenges and Technologies. IEEE Sensors Reviews, 2025, 2, pp. 1-16.

[4] Thango B A. Winding Fault Detection in Power Transformers Based on Support Vector Machine and Discrete Wavelet Transform Approach. Technologies, 2025, 13(5), pp. 200.
[5] Prejbeanu R G. A Sensor-based system for fault detection and prediction for EV multi-level converters. Sensors, 2023, 23(9), pp. 4205.
[6] Ruzimov S, Zhang J, Huang X, et al. Detection of Inter-Turn Short-Circuit Faults for Inverter-Fed Induction Motors Based on Negative-Sequence Current Analysis. Sensors, 2025, 25(15), pp. 4844.
[7] Shen H, Tang X, Luo Y, et al. Online open-circuit fault diagnosis for neutral point clamped inverter based on an improved convolutional neural network and sample amplification method under varying operating conditions. IEEE Transactions on Instrumentation and Measurement, 2024, 73, pp. 1-12.
[8] Yang X, Tu Y, Yuan Z, et al. Intelligent overheating fault diagnosis for overhead transmission line using semantic segmentation. High Voltage, 2024, 9(2), pp. 309-318.
[9] Laaziz M, Nicolau F, Ghanes M, et al. Fault Detection, Isolation, and Estimation for a Three-Phase Grid Connected DC-AC Inverter With LCL Filters. IEEE Control Systems Letters, 2024, 8, pp. 1769-1774.
[10] Qiu Z, Li J, Zhu X, et al. Detection of Crimping Defects in X-DR Images of Strain Clamps Based on Multi Attention Mechanism Fusion Network. IEEE Transactions on Power Delivery, 2024, 39(4), pp. 2125-2137.
[11] Shakiba F M, Azizi S M, Zhou M, et al. Application of machine learning methods in fault detection and classification of power transmission lines: a survey. Artificial Intelligence Review, 2023, 56(7), pp. 5799-5836.
[12] Guo B, Li Q, Jiang W, et al. A deep sensing system for monitoring the health status of transmission line equipment based on self-powered sensors. IEEE Sensors Journal, 2023, 23(18), pp. 20834-20844.
[13] Luo P, Wang B, Wang H, et al. An ultrasmall bolt defect detection method for transmission line inspection. IEEE Transactions on Instrumentation and Measurement, 2023, 72, pp. 1-12.
[14] Dadashizadeh Samakosh J, Enayati F. Operation recommendations for tension joints and clamps on a 63 kV overhead transmission line conductor based on experimental tests. Electric Power Components and Systems, 2023, 51(7), pp. 639-655.
[15] Chen B, Zhang W, Wang F, et al. Development of automatic arc sag measurement equipment for tensioned line tightening construction on overhead transmission lines. Scientific Reports, 2024, 14(1), pp. 19253.
[16] Luo Y, Gao C, Wang D, et al. Predictive model for sag and load on overhead transmission lines based on local deformation of transmission lines. Electric Power Systems Research, 2023, 214, pp. 108811.
[17] Li P, Fan Y, Liu Z, et al. Application status and development trend of intelligent sensor technology in the electric power industry. IET Science, Measurement & Technology, 2024, 18(4), pp. 145-162.
[18] Mai Y, Xing Y, Ye Z, et al. Current reconstruction and sag/wind deflection monitoring of transmission lines by magnetic sensing. IEEE Transactions on instrumentation and measurement, 2024, 73, pp. 1-13.
[19] Lin Y, Zhou T, Wang Z. A High-Reliable Wireless Sensor Network Coverage Scheme in Substations for the Power Internet of Things. Symmetry, 2023, 15(5), pp. 1020.
[20] Pelini J, Russo S D, Garcia I L, et al. New silicon-based micro-electro-mechanical systems for photo-acoustic trace-gas detection. Photoacoustics, 2024, 38, pp. 100619.
[21] Gazzola C, Corigliano A, Zega V. Total harmonic distortion estimation in piezoelectric micro-electro-mechanical-system loudspeakers via a FEM-assisted reduced-order-model. Mechanical Systems and Signal Processing, 2025, 222, pp. 111762.
[22] Rzayeva S V, Guseynova I A. Application of automatic monitoring and control systems for reliability of power transmission lines. Reliability: Theory & Applications, 2024, 19(2 (78)), pp. 64-69.
[23] Pang G, Zhang Z, Hu J, et al. Analysis of Failures and Protective Measures for Core Rods in Composite Long-Rod Insulators of Transmission Lines. Energies, 2025, 18(12), pp. 3138.
[24] Boulkroune A, Hamel S, Zouari F, et al. Output-Feedback Controller Based Projective Lag-Synchronization of Uncertain Chaotic Systems in the Presence of Input Nonlinearities. Mathematical Problems in Engineering, 2017, 2017(1), pp. 8045803.
[25] Boulkroune A, Zouari F, Boubellouta A. Adaptive fuzzy control for practical fixed-time synchronization of fractional-order chaotic systems. Journal of Vibration and Control, 2025, pp. 10775463251320258.
[26] Zouari F, Saad K B, Benrejeb M. Adaptive backstepping control for a class of uncertain single input single output nonlinear systems. 10th International Multi-Conferences on Systems, Signals & Devices 2013 (SSD13). IEEE, 2013, pp. 1-6.
[27] Zouari F, Saad K B, Benrejeb M. Robust neural adaptive control for a class of uncertain nonlinear complex dynamical multivariable systems. International Review on Modelling and Simulations, 2012, 5(5), pp. 2075-2103.
[28] Rigatos G, Abbaszadeh M, Sari B, et al. Nonlinear optimal control for a gas compressor driven by an induction motor. Results in Control and Optimization, 2023, 11, pp. 100226.
[29] Merazka L, Zouari F, Boulkroune A. High-gain observer-based adaptive fuzzy control for a class of multivariable nonlinear systems. 2017 6th International Conference on Systems and Control (ICSC). IEEE, 2017, pp. 96-102.